Discriminating movements of liquid and gas in the rabbit colon with impedance manometry.

Running title: Colonic impedance manometry

Authors: R Mohd Rosli[2], RE Leibbrandt[1], L Wiklendt[1], M Costa[1], DA Wattchow[1,2], NJ Spencer[1], SJ Brookes[1], TI Omari[2], PG Dinning[1,2]

Affiliations: 1) College of Medicine and Public Health & Centre for Neuroscience, Flinders University, South Australia, Australia.

2) Department of Gastroenterology & Surgery, Flinders Medical Centre, South Australia, Australia.

Correspondence: A/Prof Phil Dinning

Departments of Gastroenterology & Surgery

Flinders Medical Centre

South Australia 5042.

Email: phil.dinning@flinders.edu.au

Abstract and keywords

Key Messages

- High-resolution manometry has allowed us to identify motor patterns that had previously been missed or mislabeled. However, the propulsive nature of these motor patterns cannot be determined by manometry alone.
- Using a high-resolution impedance manometry catheter in an isolated rabbit colon, we have characterized the relationship the exists between pressure and impedance to identify the passage of intraluminal liquid or gas. Using the characteristic shape of the pressure/impedances signals, we developed an automated approach to identify episodes of liquid or gas transit.
- These data indicate that high-resolution impedance manometry recording may be of benefit for defining pressure/flow relationship in the human colon, where real-time monitoring of gaseous and liquid content can be difficult.

Abstract

Background High-resolution impedance manometry is a technique that is well established in esophageal motility studies for relating motor patterns to bolus flow. The use of this technique in the colon has not been established. **Methods** In isolated segments of rabbit proximal colon, we recorded motor patterns and the movement of liquid or gas boluses with a high-resolution impedance manometry catheter. These detected movements were compared to video recorded changes in gut diameter. Using the characteristic shapes of the admittance (inverse of impedance) and pressure signals associated with gas or liquid flow we developed a computational algorithm for the automated detection of these events. **Key Results** Propagating contractions detected by video were also recorded by manometry and impedance. Neither pressure or admittance signals alone could distinguish between liquid and gas transit, however the precise relationship between admittance and pressure signals during bolus flow could. Training our computational algorithm upon these characteristic shapes yielded a detection accuracy of 87.7% when compared to gas or liquid bolus events detected by manual analysis. **Conclusions & inferences** Characterizing the relationship between both admittance and pressure recorded with high-resolution impedance manometry can not only help in detecting luminal transit in real time, but also distinguishes between liquid and gaseous content. This technique holds promise for determining the propulsive nature of human colonic motor patterns.

Keywords colonic motility, high-resolution impedance manometry, admittance, colonic transit, peristalsis.

Introduction

Colonic motor patterns mix and propel luminal contents in a controlled manner to allow for the absorption of water, electrolytes, and ultimately excrete waste. Over the past few decades, a number of different techniques have been used to monitor the transit of content through the human digestive tract. These include x-ray, scintigraphy and a range of wireless capsules.[1] In addition to these, tools have also been developed to record the contractile activity of the gut, including manometry, ultrasound and magnetic resonance imaging.[2] However despite these advances, there is still a poor understanding of the relationships that exist between the motor patterns and movement of content within the colon.[3,4] In animal studies, real time movement of luminal content recorded by fluoroscopy has been combined with colon motor patterns recorded by strain gauges attached to the serosa.[5,6] While such studies allow moment-by-moment comparison between flow and motor patterns, extended periods of radiation cannot be used in human studies.

In recent years, high-resolution impedance manometry (HRIM) has been used in the human esophagus and small bowel, to monitor real-time transit of content and the associated motor patterns[7-10]. As impedance is a measure of resistance of electrical conductivity between two electrodes, the impedance signal is influenced by the conductivity of the medium surrounding the electrodes. In general, the impedance signal will differ when in contact with liquid or gas.[11] While impedance manometry has been validated for use in the human esophagus[12] its use in the colon has not been established.

In this work, we used isolated preparations of rabbit colon and our established technique of spatiotemporal mapping [13-15] to determine the ability of a high-resolution

impedance manometry catheter to tract the movements of liquid and gas along the colon and relate these movements to the recorded motor patterns. Specifically, our three aims were to: 1) characterize the impedance changes associated with movement of intraluminal liquid and gas; 2) relate these movements to the associated pressure patterns; and 3) to develop and validate an automated approach for detection and analysis of liquid or gas bolus movements.

Materials and methods

Nine New Zealand albino rabbits (seven females) weighing 0.96 – 2.7 kg were euthanized humanely by intravenous phenobarbitone sodium injection (162.5 mg kg^{-1}) in accordance with approval by the Animal Welfare Committee of Flinders University (application number 820/12). A ventral midline incision was made to expose the peritoneal cavity. The proximal colon, containing triple- and single-teniated regions,[15] were taken from the rabbits. Each specimen was placed immediately into beakers containing warmed (36^{O}C), oxygenated Krebs solution (in mM: 118 NaCl, 4.7 KCl, 1.0 NaH_2PO_4, 25.0 $NaHCO_3$, 1.2 $MgCl_2$, 11 D-glucose, 2.5 $CaCl_2$) bubbled with 95% O_2/ 5% CO_2. Fecal material was left to spontaneously empty out of the specimen for 15 minutes. Any remaining fecal content was then gently flushed out with Krebs solution using a syringe inserted at the oral end.

Experimental set up

The experimental setup was similar to previous publications[13-15] (Figure 1). Each specimen was placed into an organ bath filled with carbogenated Krebs solution, warmed at 36^{o}C. The oral end of the specimen was tied using a thread to an opening of an “inverted T”-shaped plastic connector. The anal end was tied to an “L”-shaped connector. The impedance manometry catheter was passed through the T-connector

into the lumen of the specimen with the tip resting in the L-shaped connector at the anal end. A peristaltic pump was connected to the remaining vertical opening of the T-connector. This pump could infuse either warmed Krebs solution or ambient air, into the specimen. Parafilm wax (Parafilm “M”, Pechiney Plastic Packaging, Chicago, USA) was wrapped around the catheter and the L- and T-shaped connector to prevent leakage of luminal contents. The vertical part of the L-shaped connector was attached to an outflow tube. The end of the outflow tube was set to a given height above the segment of colon to provide backpressure. A timing light was placed on the edge of the bath and used to synchronize the video and impedance manometry recordings (see below).

Video recording of diameter changes and creation of spatiotemporal maps

A digital video camera (Canon, LEGRIA HF R606) was positioned above the specimen to record movies of colonic wall motion at 25 frames per second, in 10-minute clips. The videos were converted into spatiotemporal maps of changes in diameter (DMaps) using software developed in Matlab (Mathwork, Natick, MA, USA), described in previous publications.[13-16] Briefly, the diameter along the length of specimen was calculated for each video frame and converted into gray scale spatiotemporal diameter map (DMap). In a DMap, regions that are white represent minimal diameter, such as gut contraction (secondary to circular smooth muscle shortening), and regions that are black represent maximal diameter, such as when the gut is distended by a bolus (Figure 2A & 3A).[14-16] Based on these principles, propagating contractions and bolus presence could be easily identified on the DMap.[17]

Pressure and impedance recording

A solid-state high-resolution impedance manometry (HRIM) catheter (Sandhill Scientific, Unisensor USA Inc.) was used to record intraluminal pressure and impedance. This commercially available catheter has an outside diameter of 3mm, which increases to 5mm at each of the 32 pressure sensors. The catheter also incorporated 16 impedance segments, with sensor rings spaced evenly at 2cm intervals. The first of these rings was located 2cm from the tip of the catheter. Pressure and impedance data were acquired at 25Hz using InSIGHT^{TM} (Sandhill Scientific, Unisensor USA Inc.). Once acquired these pressure and impedance data were exported as text (*.txt) files and opened in our custom-made PlotHRM software written in Matlab and Java (Sun Microsystems, CA, USA)[18].

In keeping with our recent publications, we have used the inverse of impedance (admittance) in our analysis.[13,19,20] Based on principles of intraluminal electrical resistivity, when the impedance sensors are surrounded by air, admittance will be *low*, and when the sensors are surrounded by a saline solution, admittance will be *high*.

Experiment protocol

After the setup, the excised colon was allowed to rest in the organ bath for at least 30 minutes, after which warmed (36^{O}C) Krebs solution was infused by the peristaltic pump at 2.1ml min^{-1} until Krebs solution was observed to drip out of the outflow tube. The height of the outflow opening was then lifted by 1cm to provide back pressure to distend the colon and initiate contractile activity. The impedance manometry recording commenced and the colon was continually perfused at 2.1ml min^{-1} for a further 10 minutes. During this period the video camera positioned above the gut recorded the contractile activity.

In order to change the intraluminal infusion from Krebs to air, the inflow tubing was removed from the Krebs solution allowing ambient air to be drawn into the tubing by the peristaltic pump and then into the colon. The tip of the outflow tube was submerged into a water-filled beaker, approximately 1cm beneath the water surface, for visual confirmation of gas moving through and out of the colon. The impedance manometry continued recording throughout the change from liquid to gas infusion. Once the gas bubbles first appeared in the beaker, a second 10-minute video recording began. During all video recordings, at irregular intervals, a digital mark was placed on the impedance manometry trace synchronized with the timing light flash on the organ bath. This allowed temporal alignment of the impedance manometry recordings with the video-converted DMaps.

The alignment in space and time of impedance manometry with the DMaps occurred automatically using custom software written in Matlab by two of the authors (RL, LW). This allowed for all three data parameters (admittance, pressure, and diameter) to be viewed together as line tracings, spatiotemporal maps or combinations of the two.

Definition and manual identification of events

Propagating contractions: DMaps were used as the “gold standard” in identifying colonic motor events. Propagating contractions were readily seen as oblique white streaks that followed after darker oblique streaks, which were indicative of propagated luminal distension from bolus transit (Figure 2A and 3A). In this study, we analyzed the propagating contractions that extended through the entire length of the specimen. The pressure events recorded by the manometry sensors (individual phasic pressure increases recorded by each sensor), when viewed across multiple channels formed recognizable propagating pressure events. Propagation was

confirmed if a pressure event peak occurred in four or more adjacent channels (i.e. ≥4cm).[21] If a pressure event returned to baseline before the pressure event in the adjacent channels started, then the two events were not considered part of a single propagating motor event. Similar criteria were used for the analysis of the admittance trace, although as the impedance sensors were spaced at 2 cm intervals, a propagating admittance events was defined over two or more adjacent admittance channels (i.e. ≥4cm).

Common cavity phenomenon: In some motor events, proximal propagating contractions caused simultaneous distension of the distal colon over a certain length. This simultaneous distension, was manometrically recorded as a synchronous rise of pressure events across multiple sensors along the distended segment (Figures 4B and 5B). This simultaneous segmental pressure increase and distension was previously labelled as a "common cavity" phenomenon.[14] This phenomenon was more apparent in the manometry traces than in the DMaps. Therefore, the manometry trace was used as the gold standard for common cavities. The common cavity was defined as a synchronous rise in pressure occurring over at least four adjacent channels (i.e. ≥4cm).

<u>Relationship between admittance and pressure recordings during propagating contractions and common cavities.</u>

The changes in admittance during propagating contractions or common cavities were measured as absolute admittance increase or decrease relative to peak (with liquid infusion) or nadir admittance (with gas infusion). Standardized admittance and pressure data over a 20-second time window, centered on peak (during liquid infusion) or nadir (during gas infusion) admittance, were aligned over all manually identified propagating contractions and common cavities. The mean data "profiles"

for admittance and pressure in both liquid and gas conditions were extracted to show the relationship between admittance and pressure during propagating contractions and common cavities (Figure 6).

Automatic analysis

In esophageal studies, a subject can be prompted to swallow on command and analysis can be focused upon that event. In contrast, colonic propagating activity is not under voluntary control. The recording must usually be of a longer duration (many hours) and movements of content can occur at any time. Therefore, an important aim of this study was the development of an automated approach to identify periods of liquid and gas bolus movement. This software was created by one of the authors (RL) in Matlab and Java (Sun Microsystems, CA, USA), and formed part of the GutMiner software package. The software consisted of two procedures:

1) The *threshold procedure* classified the admittance data using a simple threshold value. Admittance values over the threshold were classified as liquid, while values below the threshold were classified as gas. In the first step, the admittance data from eight of the nine rabbits was scaled between 0 and 1 for each individual recording channel, and a threshold value was selected as the value that would yield optimal classification accuracy of luminal content. This threshold value was then used to classify the admittance data from the ninth rabbit. This process was repeated eight additional times, each time choosing a different rabbit as the excluded “ninth” rabbit (“leave-one-subject-out cross validation”)[22] and the mean accuracy was calculated over all nine experimental animals.
2) The *shapelet procedure* identified recurrent patterns in admittance and pressure that were differentially associated with either liquid or gas bolus.

These patterns were represented as distinctive “shapes” embedded in the aligned time series data and can be visualized (Figure 7). The procedure was based on the Shapelets approach used in time series data mining.[23 24] Using “leave-one-subject-out cross validation”, admittance-pressure patterns that reliably occurred with liquid bolus or gas bolus respectively were extracted. Subsequently, all approximate matches of liquid-associated and gas-associated patterns were located in the data from the left-out rabbit, and used to classify the matched data into liquid or gas bolus. The percentage of correctly classified samples out of all matched samples was calculated. In addition, the degree of correspondence between shapelet procedure and manual identification of motor activity was evaluated. Thus every manually-identified propagating contraction that also showed a shapelet match for the appropriate bolus in at least 3 consecutive admittance channels (≥6cm) was counted as having been automatically identified, and the percentage of automatically-identified contractions out of all contractions was calculated.

Statistical data analysis

All values were calculated automatically using the custom Matlab software. Median (range) were expressed for data that did not follow a normal distribution, and for other data the mean (± 95% confidence interval) was reported, unless stated otherwise. Mann-Whitney test was used to compare between changes in admittance during propagating contractions and common cavities. The same statistical test was also used to compare the peak pressure amplitudes and velocities of propagating contractions associated with liquid and gas boluses. A p-value of less than 0.05 ($p<0.05$) was considered as statistically significant. A total recording of 180 minutes

of liquid and gas infusion (10 min for each medium in each rabbit, n=9) was used for analysis.

Results

General observations confirmed intuitive expectations regarding admittance traces. Admittance is the inverse of impedance, so formation of a thick column of fluid (by distension of propulsion) always causes a rise in admittance. A thick column of gas distending the lumen was consistently associated with very low admittance. Admittance of the rabbit colonic mucosa typically lay between the peak admittance of liquid content and the nadir admittance of a column of gas. These simple associations explain many of the following observations. A summary of admittance changes during identified propagating contractions and common cavities in different medium is presented in Table 1.

During liquid infusion, a total of 60 propagating contractions (mean = 6.67 ± 3.47 /10 min) were identified on the DMaps, all of which were also detected by both manometry and admittance. In addition, there were 65 common cavity phenomena (mean = 7.22 ± 4.89 /10 min) identified in manometry traces, all of which were observed distal to a propagating contraction (Figure 4). Common cavities also affected admittance traces but were not evident in DMaps.

During gas infusion, there were 78 propagating contractions (mean = 8.78 ± 2.5 /10 min) detected on the DMap and by both manometry and admittance. In addition, 46 common cavities occurred during gas infusion (mean = 5.11 ± 4.48 /10 min). Again, while evident on the manometry trace these were not readily apparent in DMaps. Gas filled common cavities also occurred consistently distal to a propagating contraction (Figure 5).

There was no difference between the mean peak pressure amplitude of propagating contractions associated with the transit of liquid (11.53 ± 0.71 mmHg) and gas (13.37 ± 0.75) boluses (p=0.06). The mean velocity of propagating contractions associated with liquid boluses (25.02 ± 2.74 mm s^{-1}) was slightly higher than velocity of the propagating contractions associated with gas boluses (21.05 ± 2.17 mm s^{-1}) (p<0.01).

Admittance and pressure relationship with liquid bolus

Changes in admittance and pressure during a single propagating contraction of a liquid bolus can be seen in Figure 2. Characteristic, averaged changes are shown in Figure 6A. In general, the following sequence occurred during the passage of a liquid bolus: Admittance started to increase as a column of fluid built up, due to the upstream contraction. It peaked just before the pressure started to rise, due to the arrival of the wavefront of the propagating contraction. As pressure rose, admittance began to fall, because the contraction narrowed the lumen and thus made the column of fluid narrower. The nadir of admittance occurred close to when pressure peaked during a lumen-occlusive contraction. Admittance then started to rise as pressure fell and fluid partially re-filled the segment.

During a common cavity, there was a simultaneous increase in admittance distributed along the specimen containing the continuous column of Krebs liquid (Figure 4C). The pressure rise in the common cavity occurred before peak admittance (Figure 6B).

Admittance and pressure relationship with gas bolus

As expected, propulsion of a gas bolus caused very different patterns of pressure and admittance from passage of liquid. During a propagating contraction, gas bolus

movement was characterized by an initial large drop in admittance which reach a nadir prior to a rise in the pressure, due to the non-viscous gas moving well ahead of the advancing contraction (Figures 3 and 6C). As pressure then started to increase, the admittance began to rise, with a return to baseline coinciding with the pressure peak during a lumen-occlusive contraction.

When infusion of gas caused a common cavity, the drop in admittance from baseline (due to accumulating gas) was nearly synchronous with the increasing intraluminal pressure, with the nadir point occurring close to the peak intraluminal pressure (Figures 5 and 6D). The admittance then rose back towards baseline as the pressure began to drop, reflecting gas leaving the distal end of the gut segment.

Automatic classification of gas and liquid bolus

The automatic threshold procedure yielded a normalized admittance threshold of 0.71, meaning that the lower 71% of the admittance value range for each recording channel over the entire recording period was classified as gaseous content. The upper 29% was classified as liquid content. Mean classification accuracy, compared to known content was 94.2%.

The automated shapelet procedure identified sets of aligned, averaged admittance-pressure events for both gas and liquid boluses (example patterns for liquid and gas, of a fixed duration of 9 seconds, are shown in Figure 7). These events accounted for 26.7% of the duration of all recordings. Classification accuracy using shapelets' patterns for known content was 84.0%.

A total of 138 full-length propagating contractions (60 during liquid and 78 during gas infusion), that spanned along the whole specimen were identified in DMaps. The shapelet procedure automatically identified 46 out of 60 (76.7%) of

manually identified propagating contractions evoked by liquid. This procedure also identified 75 out of 78 (96.2%) of manually-identified propagating contractions caused by gas infusion, giving a total accuracy of 121 out of 138 (87.7%). All automatically identified propagating contractions had admittance and pressure events that occurred across at least 3 consecutive admittance recording channels (at least 6cm or more).

Discussion

This work has applied impedance manometry under controlled conditions in isolated preparations of rabbit colon to establish a reliable method to distinguish motor patterns temporally associated with liquid or gas movement. Our study design allowed for highly controlled infusion of either liquid or gas contents and their movements could be reliably recorded by video. Identified propagating contractions on spatiotemporal maps of diameter (DMaps) could then be related in space and time to the impedance manometry recordings. While both the manometry and impedance sensors detected the transit of luminal content, individually neither technique could distinguish between liquid or gas bolus. However, when the pressure and admittance signals were combined the transit of the two different luminal contents could be determined. During the passage of a liquid bolus (Figures 2 and 6A), the rise in admittance reflected the increase in conductivity of the column of Krebs solution surrounding the impedance sensors. The subsequent drop in admittance was a result of the Krebs solution passing the sensors and their subsequent contact with the mucosa during a lumen-occlusive contraction. Arrival of a poorly conducting gas bolus reduced contact between the moist colonic mucosa and the impedance sensors, causing a drop in admittance. The contraction that

followed displaced the gas, resulting in return of mucosal contact with the sensors, causing an increase in admittance.

Along with the propagated contractions, our study also revealed the regular occurrences of common cavities. These always occurred distal to propagating contractions. In a previous study involving rabbit ileum, we described two synchronous pressure events; “common cavity phenomena” and “common occluded contractions”.[14] In a common cavity, a proximal propagating contraction caused an extended length of distal gut segment to dilate simultaneously, as content moved into it. The back pressure at the anal end of the preparation resulted in synchronous pressure increase along this distended length of gut. The opposite occurred in a "common occluded contraction", where an extended length of gut simultaneously contracted, also resulting in a synchronous pressure increase. Manometrically the pressure patterns were very similar and therefore indistinguishable from one another. In this study the synchronous pressure patterns were associated with the common cavities because liquid or gas were moved into the distal region, each having distinct admittance-pressure relationship profiles (Figures 6B & 6D). Common occluded contractions were not observed in this study, possibly due to such phenomena only being present in the rabbit ileum and not in the proximal colon. However, based upon the relationship between pressure and admittance during a contraction, we would predict that admittance-pressure relationship would help to distinguish common cavities from common occluded contractions. This could be of particular interest in the human colon where pan-colonic pressurizations have recently been described.[25]

Intraluminal impedance measurement has previously been shown to be more sensitive than manometry in detecting intestinal flow within the duodenum.[9,26] In

those studies, the analysis was based on liquid flow. Our study confirmed the results of those results and in addition we have been able to detail the motor patterns and admittance changes associated with gas movements. The ability to track gas in the colon is important because most colonic manometry recording in humans are performed in a prepared colon where only small amount of liquid and gas will be present. This is especially the case after a meal where gas has been shown to move into the distal colon.[27] Accumulation of gas in the colon is clinically important because intestinal gas retention has been associated with abdominal pain and symptoms.[28,29]

Previous studies in the esophagus have described markers of bolus entry and bolus exit. These corresponded to a drop in impedance and the point of recovery of 50% from baseline impedance, respectively.[7,8,10,30] Baseline impedance or admittance can be calculated in the esophagus, because most of the time it is in a collapsed state, and distends only during peristaltic propulsion of a swallowed bolus. The colon, however, functions as a storage for content. In our study the infusion of liquid or gas caused a slow distension in the proximal colonic segment, until peristaltic contraction was triggered, at which point the bolus was propelled aborally along the specimen length. This slow distension was associated with a gradual drift in the admittance, thus the baseline needed to be adjusted frequently. Additionally, admittance signals alone cannot distinguish between liquid and gaseous boluses as the signals show large drops in both cases (Figures 2C and 3C). However, when the *timing* of the propagating admittance drop is viewed together with the propagating pressure event (detected manometrically), gas and liquid boluses are readily distinguished (Figure 6). This highlights the value of establishing the precise relationship between admittance and pressure changes.

This study has also examined the usefulness of fully automated procedures in distinguishing the different kinds of bolus. A very simple threshold-based process of classification was highly accurate in distinguishing liquid from gas bolus. It should be kept in mind that a single threshold is only usable in the controlled experimental situation of the current study, where the bolus was known to be either liquid (Krebs solution) or gas (ambient room air). In the in vivo colon, a mixture of materials will comprise the luminal content, each with its own specific conductivity. Nevertheless, the results of this study confirm that the relative level of admittance can be useful in automated identification of the type of bolus.

The shapelet-based procedure is complementary to the threshold-based procedure. It explicitly discards information about the magnitude of admittance and pressure changes, and focuses on the shape of the data over brief consecutive periods. Our results have shown that this technique also attains high accuracy in recognizing combined admittance and pressure patterns that are characteristic of liquid and gaseous boluses. It should be kept in mind that the shapelet procedure is not designed to classify all of the data, but only to identify reliable cues during bolus movement (roughly a quarter of all data in the current study). The procedure showed promise in automatically finding most of the propagating contractions that had been identified manually by a researcher. The patterns identified by the shapelet procedure corresponded closely to the average profiles that were extracted from the manually identified contractions, providing independent support for our emerging picture of how admittance and pressure change during passage of a liquid or gas bolus in the colon.

There are some obvious limitations to this study. Our protocol described findings that were based on the movement of pure liquid or pure gas boluses only. In

a "prepared" human colon in vivo, where most manometric procedures are performed, there is a mixture of liquid and gas. We attempted to simulate such a mixture by alternating between infusion of Krebs solution and air. However, this only led to alternating short columns of air or liquid in the preparation, rather than a true mixture of content. This was probably due to the relatively small luminal diameter of the rabbit colon, made even smaller with intubated the catheter. When analysis was performed on these data we simply moved from a liquid to gas profile. In addition, in the rabbit colon, all propagating contractions were lumen-occlusive and moved the content towards the anal end of the preparation. Such activity did not promote the mixing of content. Whether such occlusion occurs in the human colon is yet to be determined, furthermore the human colon has a considerably larger diameter which may allow more effective mixing.

We also acknowledge that in a normal physiological setting the human distal colon would normally contain solid feces, and this would influence the impedance manometry recordings. However, in our institution and many others, the protocol for the placement of colonic manometry catheters requires a full bowel preparation and all data is also collated within 6 hours of catheter placement. Therefore, solid stool is not present during our recording.

Finally, our recordings were made in a colon will all extrinsic innervation removed and this will have an effect upon the colonic motor patterns. However, we have shown in the human colon that motor patterns recorded in vivo can also be record ex vivo.[31] Furthermore, despite the disconnection from the extrinsic innervation, the isolated animal colon is still able to generate propulsive motor patterns. We demonstrated this in our current study and previously we have shown that the propulsive nature of the motor patterns can be influenced by the luminal

content[17] Therefore, regardless of the potential change in motor patterns with the removal of extrinsic nerves, we were still able to determine the relationships that exist between the admittance and pressure signal in relation to the transit of liquid or gas.

In summary, these data show that impedance manometry can be used to distinguish liquid from gas bolus movements in the rabbit colon. Future studies will be required to determine the effect of mixed contents on admittance-pressure relationship and how these relationships relate to non-lumen occlusive contractions. While detailed studies utilizing high-resolution impedance manometry in humans are still to be conducted, these data suggest that the technique may be able to improve our understanding of the functional role of colonic motor patterns.

Acknowledgements, funding and disclosures

Funding:

1) R.M.R. is a recipient of the Flinders Medical Centre Clinicians Trust scholarship
2) The study was funded by ARC Discovery grant (12/14 DP120102192 M Costa) and conducted in the laboratory of N.J.S. with project grant support provided by NHMRC (Project No. 1067355).

Disclosures: No conflict of interests to declare

Author contributions: R.M.R., M.C. and P.G.D. conception and design of research; R.M.R. performed experiments; R.M.R., R.E.L. and L.W. analyzed data; R.M.R., T.I.O., M.C. and P.G.D. interpreted results; R.M.R and R.E.L. drafted the manuscript; R.M.R., T.I.O., M.C., N.J.S, D.A.W., S.J.B. and P.G.D edited and revised the manuscript.

References

1. Szarka LA, Camilleri M. Methods for the assessment of small-bowel and colonic transit. *Semin Nucl Med.* 2012;42(2):113-123.
2. Dinning PG, Arkwright JW, Gregersen H, O'Grady G, Scott SM. Technical advances in monitoring human motility patterns. *Neurogastroenterol Motil.* 2010;22(4):366-380.
3. Cook IJ, Furukawa Y, Panagopoulos V, Collins PJ, Dent J. Relationships between spatial patterns of colonic pressure and individual movements of content. *Am J Pysiol Gastrointest Liver Physiol.* 2000;278:G329-G341.
4. Dinning PG, Szczesniak MM, Cook IJ. Proximal colonic propagating pressure waves sequences and their relationship with movements of content in the proximal human colon. *Neurogastroenterol Motil.* 2008;20(5):512-520.
5. Hipper K, Ehrlein HJ. Motility of the large intestine and flow of digesta in pigs. *Res Vet Sci.* 2001;71(2):93-100.
6. Bedrich M, Ehrlein HJ. Motor function of the large intestine and flow of digesta in sheep. *Small Rumin Res.* 2001;42:141-155.
7. Imam H, Shay S, Ali A, Baker M. Bolus transit patterns in healthy subjects: a study using simultaneous impedance monitoring, videoesophagram, and esophageal manometry. *Am J Physiol Gastrointest Liver Physiol.* 2005;288(5):G1000-1006.
8. Omari TI, Rommel N, Szczesniak MM, et al. Assessment of intraluminal impedance for the detection of pharyngeal bolus flow during swallowing in healthy adults. *Am J Physiol Gastrointest Liver Physiol.* 2006;290(1):G183-188.

9. Imam H, Sanmiguel C, Larive B, Bhat Y, Soffer E. Study of intestinal flow by combined videofluoroscopy, manometry, and multiple intraluminal impedance. *Am J Physiol Gastrointest Liver Physiol.* 2004;286(2):G263-G270.

10. Szczesniak MM, Rommel N, Dinning PG, Fuentealba SE, Cook IJ, Omari TI. Optimal criteria for detecting bolus passage across the pharyngo-oesophageal segment during the normal swallow using intraluminal impedance recording. *Neurogastroenterol Motil.* 2008;20(5):440-447.

11. Omari TI, Dejaeger E, Van Beckevoort D, et al. A method to objectively assess swallow function in adults with suspected aspiration. *Gastroenterology.* 2011;140:1454-1463.

12. Nguyen H, Silny J, Matern S. Multiple intraluminal electrical impedancometry for recording of upper gastrointestinal motility: current results and further implications. *Am J Gastroenterol.* 1999;94(2):306-317.

13. Costa M, Wiklendt L, Arkwright JW, et al. An experimental method to identify neurogenic and myogenic active mechanical states of intestinal motility. *Front Syst Neurosci.* 2013;7:7.

14. Dinning PG, Arkwright JW, Costa M, et al. Temporal relationships between wall motion, intraluminal pressure, and flow in the isolated rabbit small intestine. *Am J Physiol Gastrointest Liver Physiol.* 2011;300(4):G577-585.

15. Dinning PG, Costa M, Brookes SJ, Spencer NJ. Neurogenic and myogenic motor patterns of rabbit proximal, mid, and distal colon. *Am J Physiol Gastrointest Liver Physiol.* 2012;303(1):G83-92.

16. Hennig GW, Costa M, Chen BN, Brookes SJ. Quantitative analysis of peristalsis in the guinea-pig small intestine using spatio-temporal maps. *The Journal of physiology.* 1999;517 (Pt 2):575-590.

17. Costa M, Wiklendt L, Simpson P, Spencer NJ, Brookes SJ, Dinning PG. Neuromechanical factors involved in the formation and propulsion of fecal pellets in the guinea-pig colon. *Neurogastroenterol Motil.* 2015;27(10):1466-1477.

18. Dinning PG, Hunt LM, Arkwright JW, et al. Pancolonic motor response to subsensory and suprasensory sacral nerve stimulation in patients with slow-transit constipation. *Br J Surg.* 2012;99(7):1002-1010.

19. Omari TI, Ferris L, Dejaeger E, Tack J, Vanbeckevoort D, Rommel N. Upper esophageal sphincter impedance as a marker of sphincter opening diameter. *Am J Physiol Gastrointest Liver Physiol.* 2012;302(9):G909-913.

20. Cock C, Besanko L, Kritas S, et al. Maximum upper esophageal sphincter (UES) admittance: a non-specific marker of UES dysfunction. *Neurogastroenterol Motil.* 2016;28(2):225-233.

21. Dinning PG, Wiklendt L, Maslen L, et al. Quantification of in vivo colonic motor patterns in healthy humans before and after a meal revealed by high-resolution fiber-optic manometry. *Neurogastroenterol Motil.* 2014;26(10):1443-1457.

22. Shenasa M, Hindricks G, Borggrefe M, Breithardt G. *Cardiac Mapping.* 3rd Edition ed. Oxford UK: Blackwell Publishing Ltd; 2009.

23. Mueen A, Keogh E, Young N. Logical-shapelets: an expressive primitive for time series classification. *Proceedings of the 17th ACM SIGKDD international conference on knowledge discovery and data mining.* 2011:1154-1162.

24. Rakthanmanon T, Keogh E. Fast shapelets: a scalable algorithm for discovering time series shapelets. *Proceedings of the 2013 SIAM international conference on data mining.* 2013:668-676.

25. Corsetti M, Pagliaro G, Demedts I, et al. Pan-Colonic Pressurizations Associated With Relaxation of the Anal Sphincter in Health and Disease: A New Colonic Motor Pattern Identified Using High-Resolution Manometry. *Am J Gastroenterol.* 2017;112(3):479-489.

26. Chaikomin R, Wu KL, Doran S, et al. Concurrent duodenal manometric and impedance recording to evaluate the effects of hyoscine on motility and flow events, glucose absorption, and incretin release. *Am J Physiol Gastrointest Liver Physiol.* 2007;292(4):G1099-1104.

27. Perez F, Accarino A, Azpiroz F, Quiroga S, Malagelada JR. Gas distribution within the human gut: effects of meals. *Am J Gastroenterol.* 2007;102:842-849.

28. Serra J, Azpiroz F, Malagelada JR. Mechanisms of intestinal gas retention in humans: impaired propulsion versus obstructed evacuation. *Am J Physiol Gastrointest Liver Physiol.* 2001;281:G138-G143.

29. Bendezu RA, Barba E, Burri E, et al. Intestinal gas content and distribution in health and in patients with functional gut symptoms. *Neurogastroenterol Motil.* 2015;27(9):1249-1257.

30. Sifrim D, Silny J, Holloway RH, Janssens JJ. Patterns of gas and liquid reflux during transient lower oesophageal sphincter relaxation: a study using intraluminal electrical impedance. *Gut.* 1999;44:47-54.

31. Dinning PG, Sia TC, Kumar R, et al. High-resolution colonic motility recordings in vivo compared with ex vivo recordings after colectomy, in patients with slow transit constipation. *Neurogastroenterol Motil.* 2016;28(12):1824-1835.

Tables

	LIQUID BOLUS admittance change (range), in miliSiemens		**GAS BOLUS** admittance change (range), in miliSiemens	
	Rise	Fall	Rise	Fall
PROPAGATING CONTRACTION	0.29* (0.003–2.90)	0.55* (0.04–3.25)	1.07* (0.008–3.69)	0.68* (0.03–3.29)
COMMON CAVITY	0.17 (0.007–1.81)	0.30 (0.02–2.00)	0.49 (0.006–2.96)	0.39 (0.02–3.47)

Table 1. Summary of admittance changes during propagating contractions and common cavities. The changes (rise/fall) in admittance during propagating contractions were significantly larger than the admittance changes that occurred during common cavities within respective mediums (* = $p<0.01$). Statistical analysis was performed using Mann-Whitney test.

Figure legends

Figure 1. A schematic diagram of the experimental set up. The high-resolution impedance manometry catheter was placed within the lumen of the excised rabbit colon. The oral end of the specimen was attached to an inflow tube where liquid (Krebs solution) or gas (ambient room air) was infused using a peristaltic pump and luminal content was expelled at the outflow tube. A video camera was placed above the specimen to record colonic wall motion.

Figure 2. A) DMap of a single full-length propagating contraction (black dashed arrow) following a passage of liquid bolus (white dashed arrow). B) DMap overlaid with pressure (green lines). Propagating pressure events are seen to occur during the propagating contraction on the DMap. C) DMap overlaid with admittance (magenta lines). Peak (maximum) admittance appears to occur during the liquid bolus passage, and decreases during the propagating contraction. D) Admittance and pressure traces aligned: admittance rises prior to a propagating pressure event and drops during the pressure event.

Figure 3. A) DMap of a single full-length propagating contraction (black dashed arrow) following a passage of gas bolus (white dashed arrow). B) Pressure traces for propagating contraction, similar to Figure 2B. C) Compared to Figure 2C, gas bolus causes a drop in admittance trace, which returns to baseline during propagating contraction. This is due to gas having poorer conductivity compared to gut mucosa. D) Admittance drops and recovers to baseline (or higher level) prior to a pressure

event. This admittance-pressure relationship is characteristically different compared to what is observed during liquid bolus (Figure 2D).

Figure 4. A) DMap of a single propagating contraction (black dashed arrow) proximally, with a distal column of liquid common cavity (white solid arrow). B) Pressure traces on DMap. Synchronous pressure events seen during a common cavity phenomenon (white box). C) Admittance traces during the common cavity phenomenon showing synchronous increase in admittance, with peak admittance occurring within the common cavity column (white box). D) Admittance and pressure traces aligned: synchronous rise in admittance prior to a common cavity phenomenon (white box) based on synchronous pressure events.

Figure 5. A) DMap of a single propagating contraction (black dashed arrow) proximally, with a distal column of gas common cavity (white solid arrow). B) Pressure traces on DMap, showing synchronous events during the common cavity phenomenon (white box), similar to Figure 4B. C) Synchronous decrease in admittance seen during the common cavity (white box), compared to increased admittance during liquid common cavity (Figure 4C). Admittance increases again when diameter becomes smaller, shown as a white streak on the DMap, and gas is expelled. D) Admittance and pressure traces overlaid: in a gas common cavity phenomenon (white box), synchronous drop in admittance occurred during the synchronous pressure peak events.

Figure 6. Relationship between admittance (magenta line) and pressure (green line) during liquid and gas infusion in different motor activities.

Figure 7. Examples of admittance-pressure “shapes” of A) liquid bolus and B) air bolus detected using the automated shapelet procedure. The automatically detected admittance-pressure relationship profile for liquid and gas boluses were comparable to the admittance-pressure profile of manually identified boluses in Figures 6A and 6C, respectively.

FIGURES

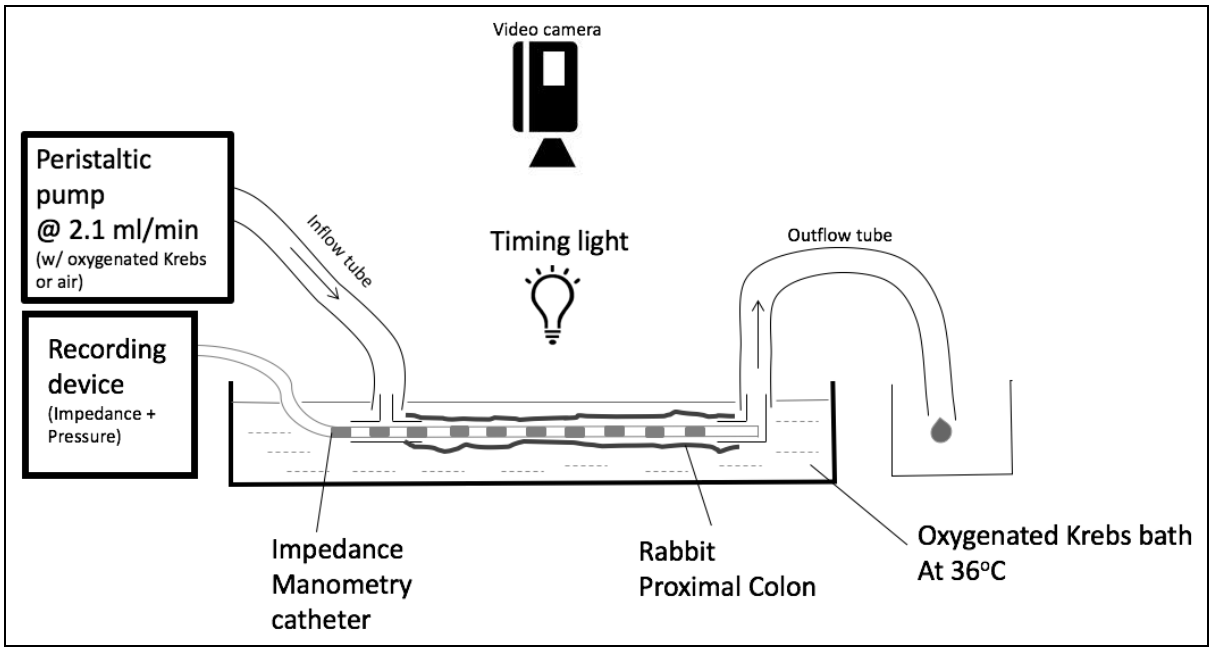

Figure 1

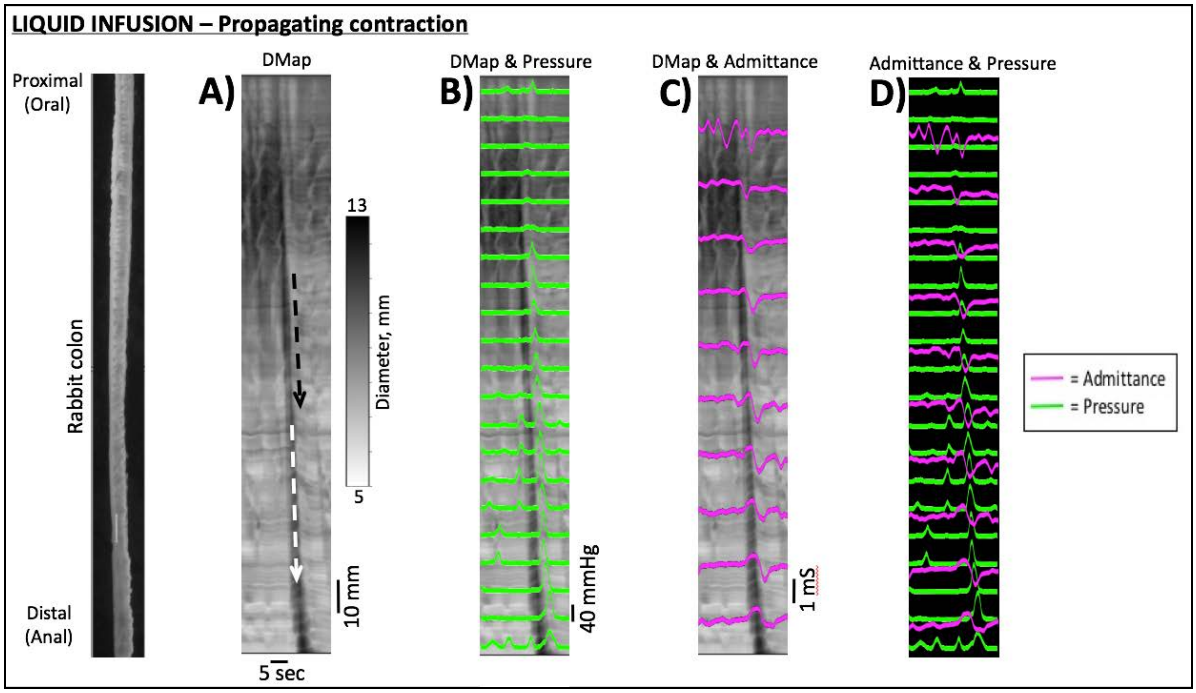

Figure 2

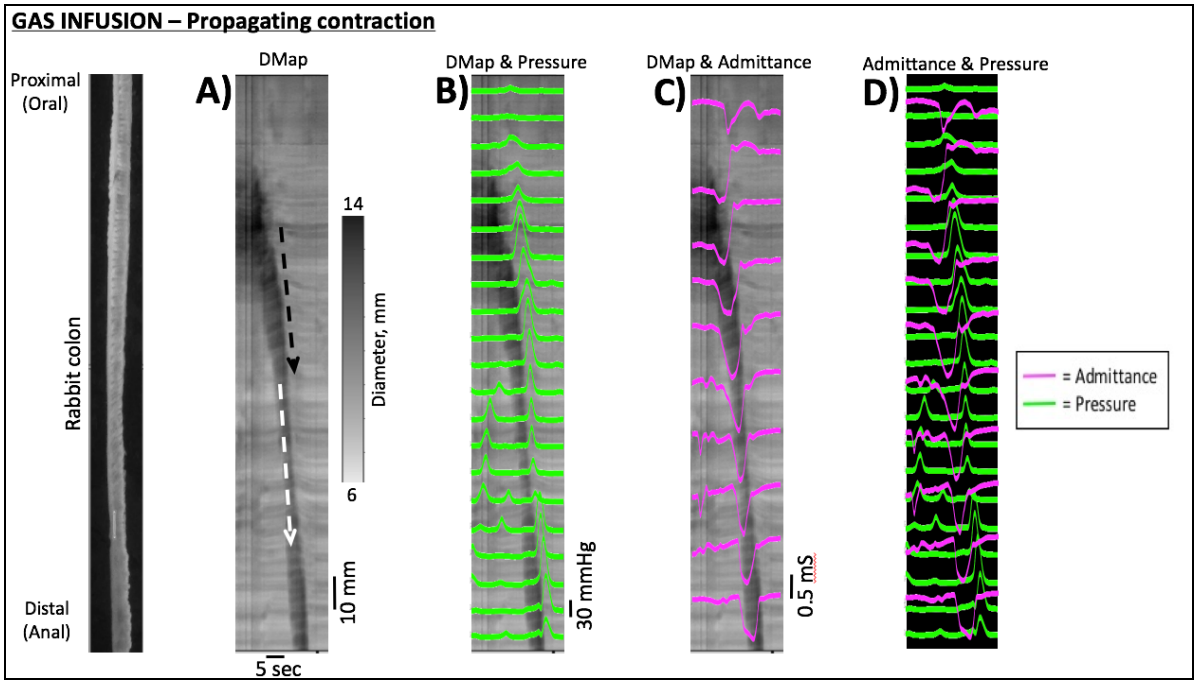

Figure 3

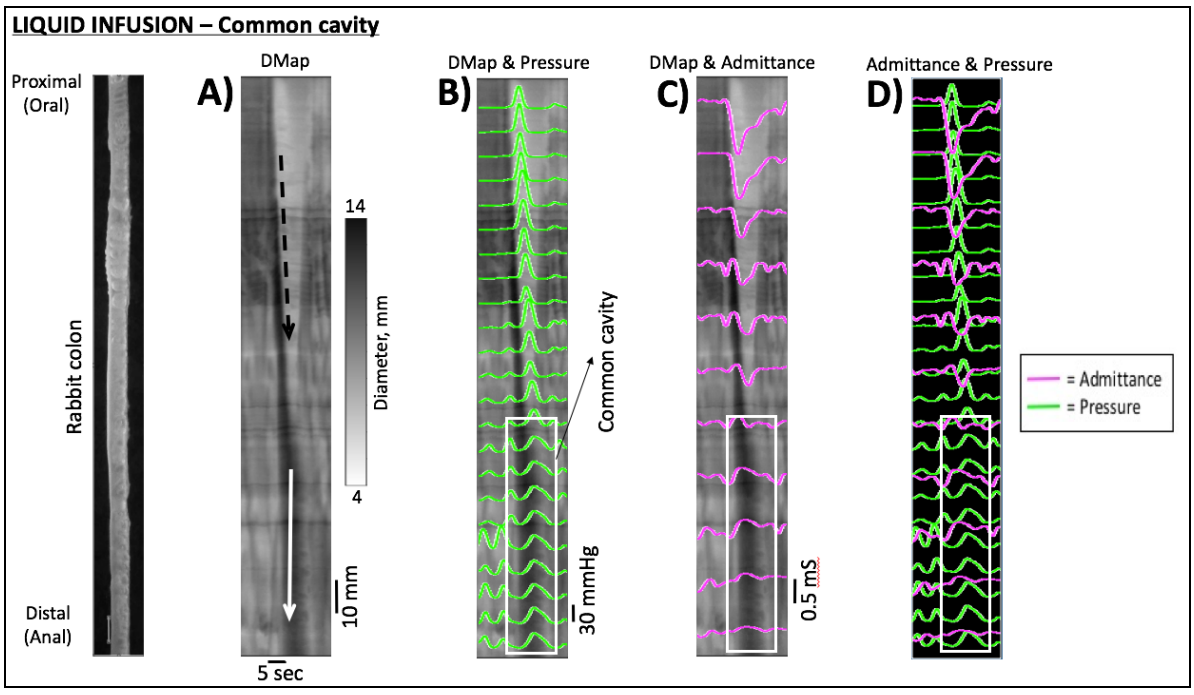

Figure 4

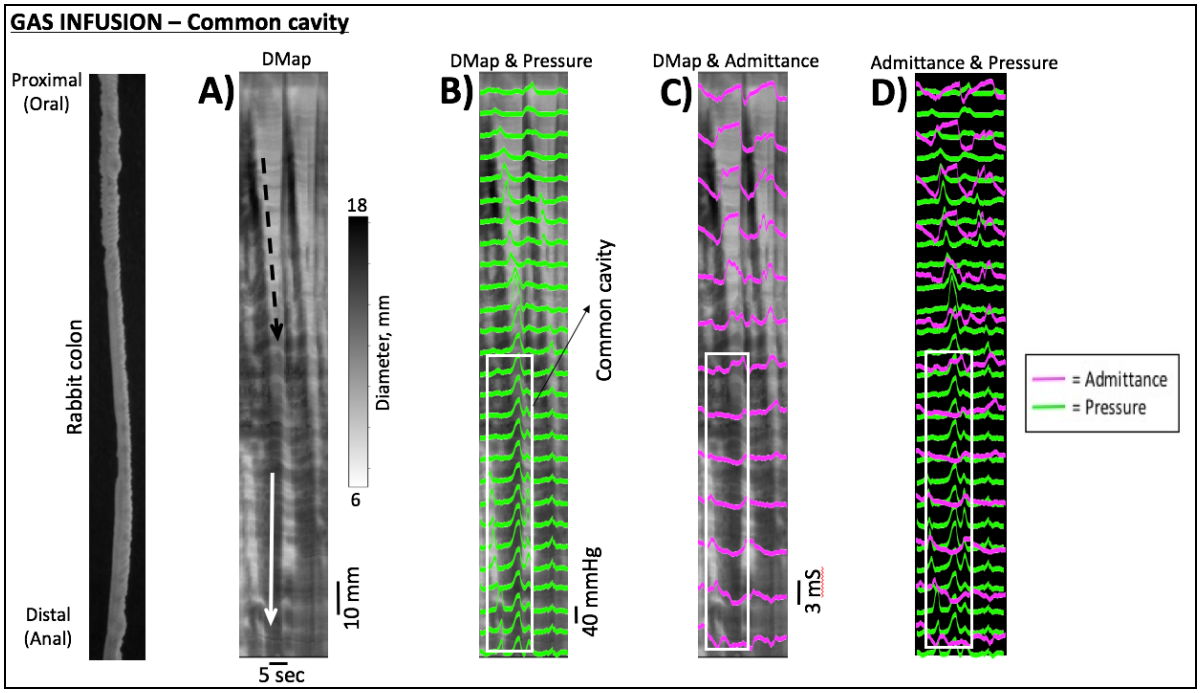

Figure 5

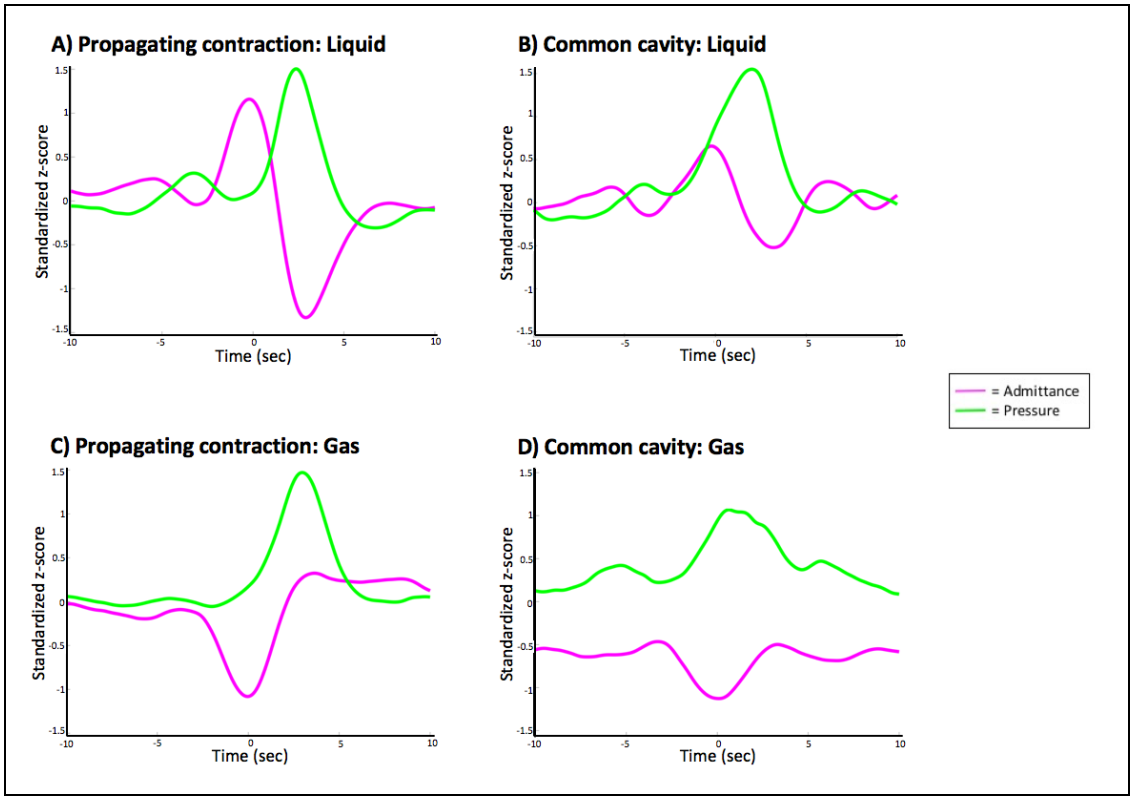

Figure 6

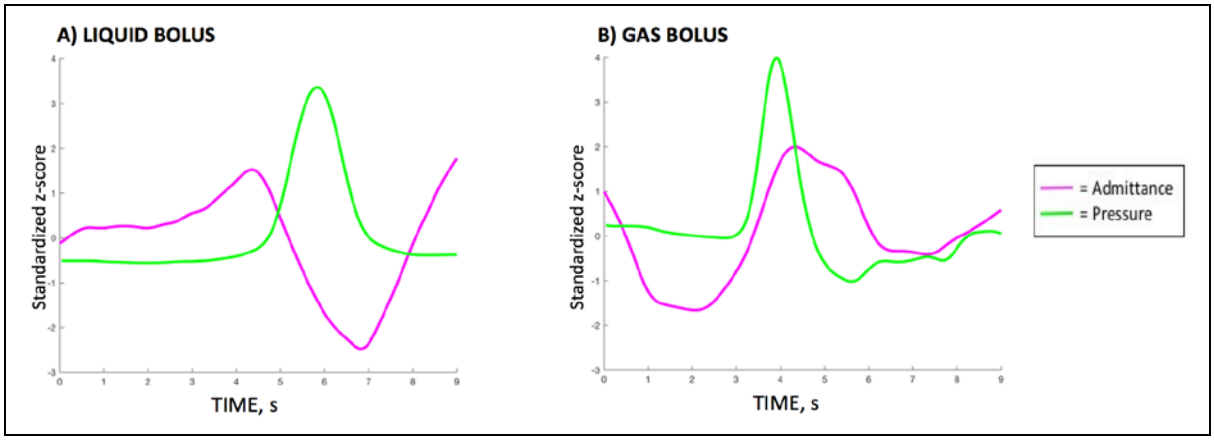
A) LIQUID BOLUS
B) GAS BOLUS
Standardized z-score
TIME, s
= Admittance
= Pressure

Figu